



## Highly efficient adsorptive removal of heavy metal ion and cationic organic pollutant from single and binary solutions using an EDTA-modified agricultural by-product-based adsorbent

Yan Liu, Qiang Gao\*, Xinyang Zhang, Shijun Xu, Bo Jin, Kaisheng Xia, Bo Han, Chenggang Zhou\*

Department of Chemistry, Faculty of Material Science and Chemistry, China University of Geosciences, Wuhan 430074, China, Tel./Fax: +86 027 6788 3731; emails: gaoqiang@cug.edu.cn (Q. Gao), cgzhou@cug.edu.cn (C.G. Zhou)

Received 28 August 2019; Accepted 13 January 2020

### ABSTRACT

Heavy metal ions and organic pollutants are hazardous contaminants commonly coexisted in various real wastewaters usually requiring complex and expensive treatment technologies. Herein, a novel low-cost agricultural by-product-based adsorbent, ethylenediaminetetraacetic acid-modified lotus seedpod (EDTA-LSP), was facilely synthesized and further utilized for the removal of toxic  $\text{Pb}^{2+}$  and malachite green (MG). In single pollutant systems, the EDTA-LSP showed considerably high adsorption capacities and rapid adsorption kinetics for  $\text{Pb}^{2+}$  (225.88  $\text{mg g}^{-1}$ ; 30 min) and MG (347.87  $\text{mg g}^{-1}$ ; 40 min), which could be rarely achieved simultaneously by many previously reported adsorbents. Particularly, the coexistence of  $\text{Pb}^{2+}$  and MG did not cause significant mutual interference, and high adsorption efficiencies for the two contaminants were still achieved. By a series of characterization analyses, it was revealed that the EDTA moieties on the adsorbent preferentially bound with  $\text{Pb}^{2+}$ , and the formed EDTA- $\text{Pb}^{2+}$  complexes could serve as effective sites for adsorption of cationic MG due to their negative charge nature. The differential binding behaviors, in turn, largely reduced the competition between the two contaminants and led to a quite satisfying coadsorption. Besides, this adsorbent could be reused several times without an obvious decrease in removal efficiencies for  $\text{Pb}^{2+}$  and MG. The low cost, simple synthesis, efficient adsorption/coadsorption, and excellent reusability indicate the EDTA-LSP is a promising adsorbent candidate for wastewater cleanup.

*Keywords:* EDTA-modified lotus seedpod; Adsorption and coadsorption; Differential binding behaviors; High adsorption performance

### 1. Introduction

Water contamination with heavy metal ions and organic pollutants has become an increasingly serious environmental problem worldwide, which poses a high risk to human beings and aquatic organisms, rendering the wastewater cleanup an urgent need [1–3]. A large number of wastewater treatment technologies have been proposed and widely used with considerable success [4–6], but most of them only show

effectiveness for removal of a single class of contaminants (either heavy metal ions or organic pollutants), possibly due to the significant difference in physical and chemical properties between the two classes of contaminants. However, heavy metal ions and organic pollutants commonly coexist in various real wastewaters. For instance, textile industrial wastewater generally contains a considerable amount of heavy metal ions [7], which act as mordant in the dyeing processes. Therefore, the development of efficient approaches

\* Corresponding authors.

to simultaneously remove heavy metal ions and organic pollutants from wastewater is of practical importance and also remains a challenge. A possible effective protocol is to upgrade an already existing successful method so that it can be competent for the simultaneous removal of both classes of contaminants.

Adsorption has been considered as one of the most preferred technologies for wastewater treatment owing to its operational simplicity, wide applicability, and eco-friendliness [8,9]. Various adsorbents such as activated carbon [10], mineral [11], resin [12], porous silica [13], industrial wastes [14], agricultural by-products [15], and nanomaterials [16] have been developed and successfully applied to the heavy metal ion and organic pollutant removal. Especially, the agricultural by-products, mainly composed of lignin and cellulose, have attracted much attention due to their abundant availability, cheapness, and biocompatibility [17,18]. Moreover, most of them are usually discarded as wastes and their disposal management is very difficult, so the use of agricultural by-products as adsorbents will be also of great significance for solving the disposal problem. A variety of agricultural by-products like wheat straw [19], rice straw [20], corn cob [21], orange peel [22], banana peel [23], and peanut hull [24] have therefore been exploited to remove heavy metal ions and organic pollutants from wastewater. In most cases, however, natural agricultural by-products have limited capacities for the removal of heavy metal ions or organic pollutants due to a lack of surface adsorption sites. Therefore, using suitable modifiers to functionalize the surfaces of agricultural by-products for boosting their adsorption abilities has become an important issue in this field.

Ethylenediaminetetraacetic acid (EDTA), a well-known chelating agent, can form highly stable chelates with various metal ions [25]. Thus, its immobilization onto solid supports is expected to generate adsorbents with excellent metal-binding properties. Many solid materials functionalized with EDTA have been therefore studied in recent years, including silica gels [26], magnetic nanoparticles [27], polymer resins [28], and agricultural by-products, etc. [29]. In particular, due to high hydroxyl content on their surfaces, the agricultural by-products can be directly modified by EDTA through a simple interfacial esterification reaction using EDTA dianhydride as a precursor. This simple but efficient synthesis makes the EDTA-modified agricultural by-products highly promising adsorbents for practical use in wastewater treatment. Nevertheless, EDTA-modified agricultural by-products, as well as other EDTA-modified materials, are mostly used for heavy metal ion removal, and only a few of them are tested as adsorbents of cationic organic pollutants. Moreover, until now, there are hardly any reports on the use of adsorbents with single EDTA functionality for simultaneous removal of heavy metal ions and organic pollutants, although some studies have recently been conducted on the functionalization of adsorbents with EDTA and additional binding sites (e.g.,  $\beta$ -cyclodextrin) for coadsorption [7].

In this work, we fabricated a novel EDTA-modified agricultural by-product based on the covalent grafting of EDTA moieties onto the lotus seedpod (LSP) and examined its unique adsorption and coadsorption properties in the removal of  $Pb^{2+}$  and cationic organic pollutant (malachite

green, MG) from single and binary solutions. It is worth noting that, the LSP is a very common agricultural by-product in South China and has recently been applied to adsorptive removal [30], but there is yet no attempt to improve the adsorption ability of LSP through EDTA modification. The  $Pb^{2+}$  and MG are selected as model pollutants because they are harmful and frequently found in various real wastewaters. Through batch adsorption investigations, it was demonstrated that the EDTA-modified LSP exhibited high adsorption capacities and rapid adsorption rates for removal of  $Pb^{2+}$  and MG in single pollutant systems. More importantly, the adsorption efficiency of EDTA-modified LSP kept almost unchanged for  $Pb^{2+}$  and only exhibited a slight decrease for MG in their coexistence, indicating that there was no significant mutual interference between the two classes of contaminants. Based on the results of characterization analyses, coadsorption mechanism was subsequently proposed. Besides, the excellent reusability of EDTA-modified LSP was also verified via cyclic operation.

## 2. Experimental

### 2.1. Raw material and chemicals

Raw LSP was received from East Lake, Wuhan, China. Acetic acid (HAc), hydrogen peroxide ( $H_2O_2$ , 30 wt.%), nitric acid, sodium hydroxide, EDTA, acetic anhydride, pyridine, dimethylsulfoxide (DMSO), malachite green (MG), and nitrate salts of metal ions ( $Pb^{2+}$ ,  $Na^+$ ,  $K^+$ ,  $Mg^{2+}$ , and  $Ca^{2+}$ ) were purchased from Sinopharm Chemical Reagent Co., Ltd. (Shanghai, China). All the chemicals and reagents employed in this work were commercially available and in analytical reagent grade. Distilled water was used throughout the experiments for solution preparation.

### 2.2. Synthesis of EDTA-LSP

Prior to synthesis, the raw LSP was converted into well-defined fibers via a facile pretreatment according to the reported procedure [31]. Briefly, the raw LSP (0.6 g) were pretreated in the mixed solution of  $H_2O_2$  (30 wt.%, 5 mL)–HAc (5 mL) under reflux for 3 h to convert into desired fibers. The fibers were collected by filtration and washed several times with water and ethanol, followed by drying at 70°C. Meanwhile, the EDTA was dehydrated into EDTA dianhydride via reaction with acetic anhydride for subsequent use [32]. Then, the EDTA-LSP was synthesized by a simple interfacial esterification reaction between LSP fibers and EDTA dianhydride, and the process could be briefly described as follows: 0.75 g of LSP fibers were immersed in the mixed solution containing dried DMSO (100 mL), EDTA dianhydride (3.46 g, 13.5 mol), and dried pyridine (5 mL). The mixture was stirred at 60°C for 20 h under nitrogen protection. Afterwards, the modified LSP fibers (EDTA-LSP) were filtered and washed with deionized water, ethyl alcohol, acetone, and  $CH_2Cl_2$  before being dried under vacuum.

### 2.3. Characterizations

Microstructure information on the samples were obtained by an optical microscope (OM, KE510-B, Seepack, China) with the magnifications of 40 $\times$  and 100 $\times$  under crossed polars,

where the images were captured by the connected computer equipment. Morphological analysis of materials were carried out using a scanning electron microscope (SEM, SU8010, Hitachi, Japan) equipped with an energy dispersive spectroscopic (EDS) micro-analysis system (OXFORD). Infrared spectra of samples were measured by a Fourier transform infrared spectrophotometer (FT-IR, VERTEX 70, Bruker, Germany) within a wavelength range of 4,000–400  $\text{cm}^{-1}$ . To acquire the surface charge features of materials involved in this work, zeta potential measurements were determined using a SurPASS 3 (Anton Paar). In order to determine the element composition and chemical valence in these samples, X-ray photoelectron spectroscopy (XPS) analysis were conducted using a scanning ESCALAB 220I-XL spectrometer with a monochromatic Al K $\alpha$  radiation (1,486.6 eV) and a step increment of 0.1 eV. The binding energies of the measured spectra were normalized on the basis of C1s peak at 284.8 eV.

#### 2.4. Adsorption and coadsorption procedures

For single pollutant system, typical adsorption process of  $\text{Pb}^{2+}$  or MG onto EDTA-LSP was carried out as follows: 5 mg of EDTA-LSP was added into 10 mL of simulated wastewater containing  $\text{Pb}^{2+}$  (100  $\text{mg L}^{-1}$ ; pH 5) or MG (100  $\text{mg L}^{-1}$ ; pH 6), and then the mixture was shaken with the speed of 200 rpm. After the adsorption was reached equilibrium, the solid fibers were separated from solution by filtration. The adsorption capacity of EDTA-LSP was calculated according to the following equation:

$$q_e = \frac{(C_0 - C_e) \times V}{m} \quad (1)$$

where  $q_e$  represents the adsorption capacity of EDTA-LSP for  $\text{Pb}^{2+}$  or MG ( $\text{mg g}^{-1}$ );  $m$  is the mass of EDTA-LSP (g);  $V$  is the volume of the  $\text{Pb}^{2+}$  or MG solution (L);  $C_0$  ( $\text{mg L}^{-1}$ ); and  $C_e$  ( $\text{mg L}^{-1}$ ) are the initial and equilibrium concentrations of  $\text{Pb}^{2+}$  or MG solution, respectively.

For  $\text{Pb}^{2+}$ -MG binary systems, the adsorption followed the process described above, expect that the contaminants  $\text{Pb}^{2+}$  (10–300  $\text{mg L}^{-1}$ ) and MG (500  $\text{mg L}^{-1}$ ) coexisted in the simulated wastewater (pH 5).

#### 2.5. Reusability process

To evaluate the reusability of EDTA-LSP in removal of  $\text{Pb}^{2+}$  or MG, 100 mg of EDTA-LSP, and 200 mL of  $\text{Pb}^{2+}$  solution (100  $\text{mg L}^{-1}$ ; pH 5) or MG solution (50  $\text{mg L}^{-1}$ ; pH 6) were added to a glass bottle. Then, the mixture-contained bottle was shaken in a shaker at 120 rpm for 30 min. Afterwards, the exhausted adsorbent was separated from the treatment solution by filtration. Then, EDTA aqueous solution (0.1  $\text{mol L}^{-1}$ ; pH 4.5) and  $\text{CH}_2\text{CH}_2\text{OH-H}_2\text{O}$  mixture (v/v = 1:1; pH 2) were used as the eluents of  $\text{Pb}^{2+}$ -adsorbed and MG-adsorbed EDTA-LSP, respectively. After regeneration, the EDTA-LSP was reused for the next cycle. Removal rate was estimated according to the following equation:

$$\text{Removal rate (\%)} = \frac{(C_0 - C_e)}{C_0} \times 100\% \quad (2)$$

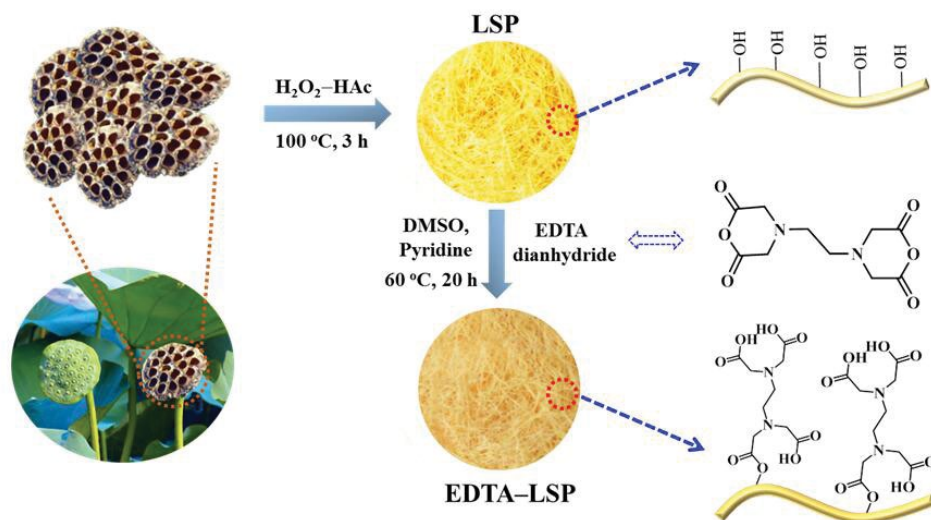
where  $C_0$  and  $C_e$  represent the initial and equilibrium concentrations of  $\text{Pb}^{2+}$  or MG ( $\text{mg L}^{-1}$ ) in treatment solutions, respectively.

### 3. Results and discussion

#### 3.1. Material characterization

As illustrated by Scheme 1, the EDTA-LSP is synthesized via a simple interfacial esterification reaction between LSP fibers and EDTA dianhydride, where the LSP fibers and EDTA dianhydride are pretreated or preprepared according to the previously reported procedures [31,32]. Then, the as-synthesized EDTA-LSP with fibrous morphology and EDTA-rich surface was developed as an adsorbent for removal of  $\text{Pb}^{2+}$  and MG from simulated wastewaters. Optical microscope and SEM measurements on LSP, EDTA-LSP,  $\text{Pb}^{2+}$ -adsorbed EDTA-LSP, and MG-adsorbed EDTA-LSP were carried out, and the obtained images are presented in Fig. 1. It can be clearly seen that the LSP sample consists of yellow fibers with diameters ranging from 100 to 200 nm and lengths of up to micrometers and the surface morphology of LSP is rough (Figs. 1a and e). The LSP-based adsorbent with well-defined fibrous structure should be somewhat advantageous over the conventional granular adsorbents because it can provide a well-balanced compromise between high adsorption efficiency and convenience for separation of adsorbent from adsorption solution. After EDTA modification and further uptake of  $\text{Pb}^{2+}$  or MG, the size and morphology of fibers do not occur obvious change (Figs. 1b–d and g–h), indicating that the LSP has a good chemical stability. Interestingly, the effectiveness of EDTA-LSP for adsorptive removal of MG can be detected visually by observing change in the color. Specifically, upon mixing of EDTA-LSP and MG solution, the EDTA-LSP fibers show a color change from yellow to green (Fig. 1d), indicating that the MG molecules are effectively enriched on the surface of EDTA-LSP via adsorption. Moreover, the remarkable ability of EDTA-LSP to remove  $\text{Pb}^{2+}$  is also verified by the EDS mapping analysis on the  $\text{Pb}^{2+}$ -adsorbed EDTA-LSP sample (Figs. 1i–m). Evidently, the Pb element has a dense and homogeneous distribution on the surface of  $\text{Pb}^{2+}$ -adsorbed EDTA-LSP sample. Taken together, our results indicate that EDTA moieties have been successfully grafted onto the surface of LSP with a high concentration level, which is expected to endow the EDTA-LSP adsorbent with high adsorption capacities for  $\text{Pb}^{2+}$  and MG removal.

To verify the changes of surface functional groups before and after grafting of EDTA on the surface of LSP, the ATR FT-IR spectra for LSP and EDTA-LSP were investigated. As shown in Fig. 2, the main adsorption peaks of LSP are located at 3,333.8; 2,899.4; 1,733.2; and 1,031.7  $\text{cm}^{-1}$ , which correspond to O–H or hydrogen bonds, C–H of  $-\text{CH}_2-$  groups, O=C=O of esters in hemicellulose, and C–N and/or C–O groups in cellulose, respectively [33–35]. After EDTA modification, these peaks are still observed. However, an absorption peak at 1,644.9  $\text{cm}^{-1}$  newly appears in the spectrum of EDTA-LSP, which can be assigned to the asymmetric stretching frequency of carboxyl groups [36], proving that EDTA graft successfully onto LSP fibers.



Scheme 1. Preparation procedure of EDTA-LSP.

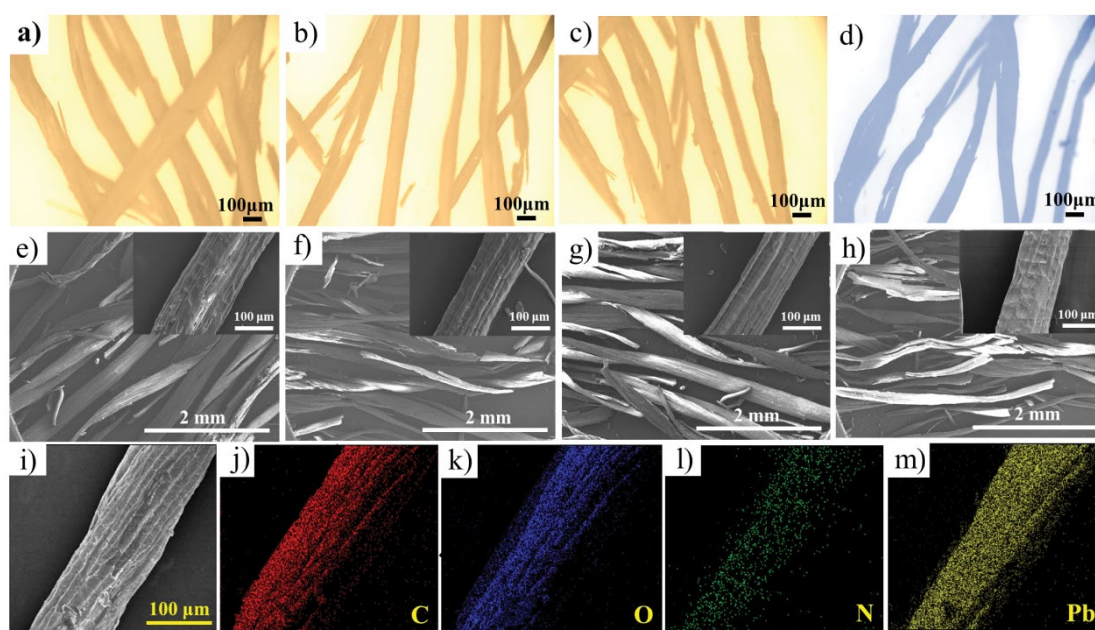


Fig. 1. Optional microscope images of LSP (a), EDTA-LSP (b),  $\text{Pb}^{2+}$ -adsorbed EDTA-LSP (c), and MG-adsorbed EDTA-LSP (d), the SEM images of LSP (e), EDTA-LSP (f),  $\text{Pb}^{2+}$ -adsorbed EDTA-LSP (g), and MG-adsorbed EDTA-LSP (h), EDS elemental mapping images of  $\text{Pb}^{2+}$ -adsorbed EDTA-LSP (i–m).

### 3.2. Adsorption of $\text{Pb}^{2+}$ and MG onto EDTA-LSP in single pollutant systems

#### 3.2.1. Effect of pH

Solution pH is a key parameter, which possibly influences the adsorption process, particularly the adsorption capacity. Thus, the effects of solution pH on the adsorption capacities of EDTA-LSP for both  $\text{Pb}^{2+}$  and MG were investigated. Given that  $\text{Pb}^{2+}$  will be partially or completely precipitated at high pH values (i.e.,  $\text{pH} > 5$ ), the solution pH for  $\text{Pb}^{2+}$  adsorption was adjusted in the range of 1–5, and the results of adsorption capacity as a function of pH are shown

in Fig. 3a. Evidently, the  $\text{Pb}^{2+}$  uptake increases continuously with the increase of solution pH and achieves a maximum value at pH 5. According to previous studies, the binding of  $\text{Pb}^{2+}$  ions to the EDTA moieties on a solid adsorbent is supposed to be driven by the surface complexation [25], and the process can be described by the following equation:



where EDTA is marked as  $\text{H}_2\text{Y}^{2-}$ . In the light of this, the pH-dependent adsorption behaviors presented in Fig. 3a is understandable. In strong acidic solutions (e.g., pH 1),

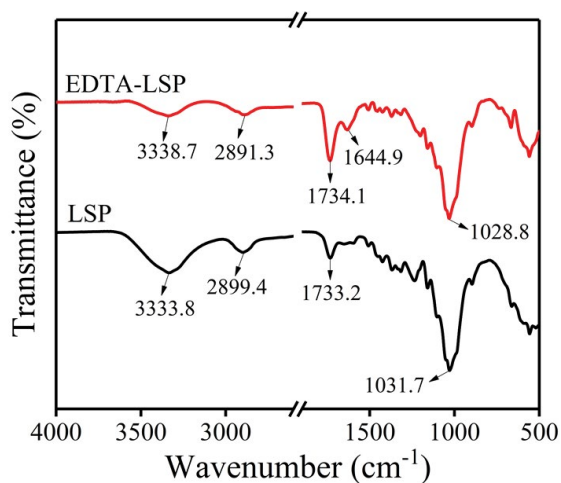


Fig. 2. FT-IR spectra of LSP and EDTA-LSP.

the  $H^+$  ion has a high concentration, which will severely inhibit the complexation between  $H_2Y^{2-}$  and  $Pb^{2+}$ , as illustrated by Eq. (3), thereby leading to a low adsorption capacity. As pH increases, the number of  $H^+$  ion decreases, and COOH groups will be gradually converted into  $-COO^-$  forms due to deprotonation, which favors the chelation between adsorbent and  $Pb^{2+}$  to achieve a high adsorption capacity [29]. Based on the obtained results, the solution pH value is set to be 5 for  $Pb^{2+}$  adsorption in the following experiments.

For MG adsorption, solution pH was adjusted over the range of 2–8, since MG would become unstable at lower or higher pH values. As shown in Fig. 3b, the adsorption of EDTA-LSP toward MG is also obviously pH-dependent. The adsorption amount increases with increasing pH from 2 to 6 and then reaches a plateau at  $pH > 6$ . This phenomenon can be well-explained as follows. Carboxyl groups of EDTA-LSP are easily protonated at low pH, which will weaken the electrostatic attraction between negatively charged adsorption sites and positively charged MG, thereby leading to a relatively low adsorption capacity. When the solution pH increases, these carboxyl groups of the adsorbent become deprotonated, which promotes the interaction of active sites

with MG and thus enhances the adsorption capacity [37]. Hence, pH 6 is selected as the optimum pH for subsequent MG adsorption experiments.

### 3.2.2. Effect of adsorbent dosage

Adsorbent dosage effect on  $Pb^{2+}$  and MG removal was investigated by adding a certain amount of EDTA-LSP (2.5–30 mg) into the pre-prepared  $Pb^{2+}$  or MG solution (10 mL, 100 mg  $L^{-1}$ ). The mixture was shaken with the speed of 200 rpm at 298.15 K for 1 h, and then the residual  $Pb^{2+}$  or MG concentration was tested to determine the adsorption capacity and removal efficiency. As shown in Figs. 4a and b, with the increase of the EDTA-LSP dosage, the removal efficiencies of  $Pb^{2+}$  and MG from the aqueous solution increase because of the increased availability of adsorption sites (i.e., EDTA moieties), which results in higher uptakes of  $Pb^{2+}$  and MG at constant concentrations. Specific adsorption capacity is a measure of the amount of  $Pb^{2+}$  or MG bound by unit weight of adsorbent. The competition of the pollutant ions or molecules for the sites available causes the decrease in the specific adsorption capacity with increment in adsorbent dosage [38].

### 3.2.3. Effect of coexisted ions

High selectivity of an adsorbent is always argued to be an important trait toward target metal ion in the presence of other metal ions. Large amounts of light metal ions such as  $Na^+$ ,  $K^+$ ,  $Ca^{2+}$ , and  $Mg^{2+}$  are concomitants along with  $Pb^{2+}$  ions in real wastewaters. Therefore, the effect of these common foreign interfering ions on adsorption capacity of EDTA-LSP toward  $Pb^{2+}$  is investigated. As shown in Fig. 5, the presence of  $Na^+$  and  $K^+$  with concentrations ranging from 0 to 10 mmol  $L^{-1}$  has no obvious influence on  $Pb^{2+}$  uptake, indicating their ineffectiveness in forming chelates with EDTA-LSP [39]. By contrast, the introduction of  $Ca^{2+}$  or  $Mg^{2+}$  into the EDTA-LSP/ $Pb^{2+}$  adsorption system can cause a slight decrease in adsorption capacity, which should be ascribed to the competitive coordination of  $Ca^{2+}$  or  $Mg^{2+}$  to carboxyl groups of EDTA-LSP [40]. Nevertheless, it should be noted that even when the  $Ca^{2+}$  or  $Mg^{2+}$  concentration (10 mmol  $L^{-1}$ ) is ten times more than that of  $Pb^{2+}$  (200 mg  $L^{-1}$ ,

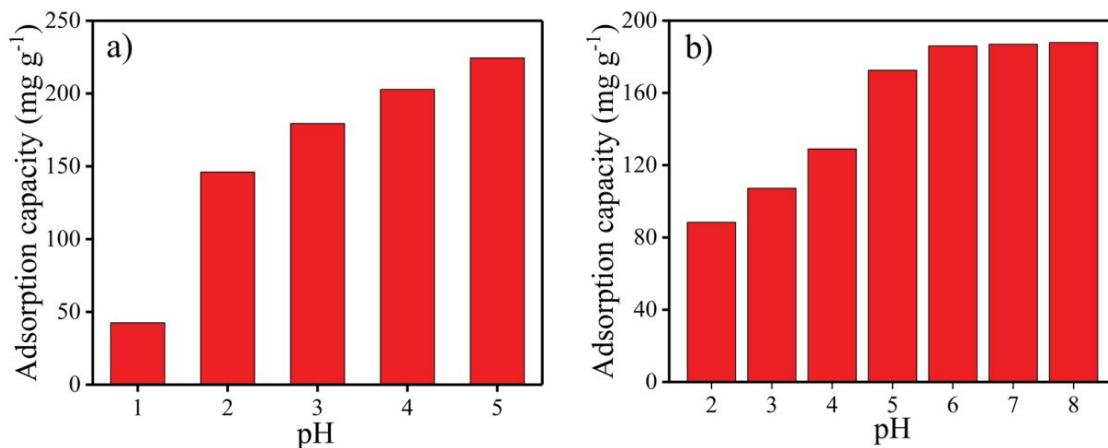


Fig. 3. The adsorption capacity of EDTA-LSP for  $Pb^{2+}$  (a) and MG (b) as a function of solution pH.

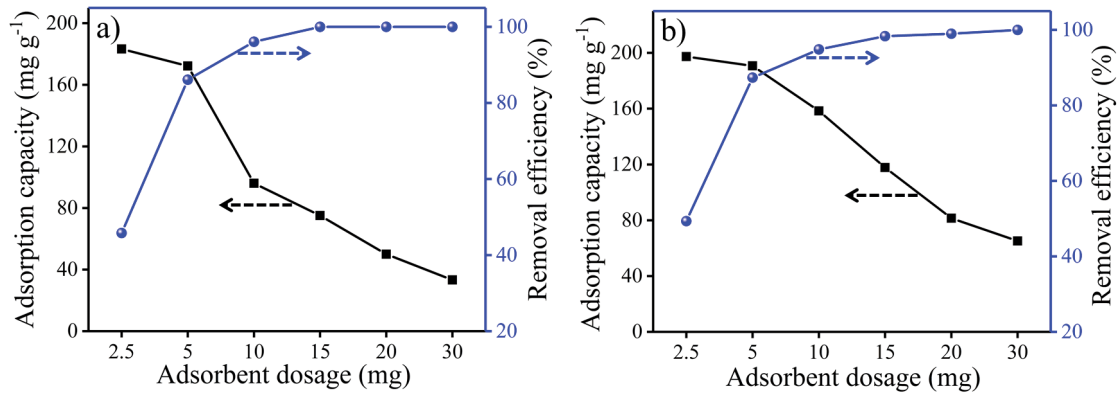


Fig. 4. Effect of adsorbent dosage on the adsorption capacities and removal efficiencies of EDTA-LSP towards Pb<sup>2+</sup> (a) and MG (b).

equivalent to 0.952 mmol L<sup>-1</sup>), the adsorption amount of EDTA-LSP for Pb<sup>2+</sup> only decreases by less than 6.3 % (Fig. 5). The result indicates that the chelation interaction between Pb<sup>2+</sup> and EDTA-LSP adsorbent is so strong that the coexistence of these interfering metal ions does not induce significant suppression on Pb<sup>2+</sup> uptake. Therefore, the novel EDTA-LSP adsorbent with strong ability to capture Pb<sup>2+</sup> from complex solutions might be applicable to real wastewater treatment.

### 3.2.4. Adsorption isotherms

Adsorption isotherms are not only valuable in describing adsorbate–adsorbent interaction but also very useful in optimizing adsorption systems [41]. Therefore, the isothermal experiments of Pb<sup>2+</sup> and MG adsorptions onto EDTA-LSP were conducted at three different temperatures (298.15, 308.15, and 318.15 K), and the results are shown in Fig. 6. It can be observed that the EDTA-LSP exhibits a high adsorption efficiency for Pb<sup>2+</sup> removal (Fig. 6a). The maximum adsorption capacities of EDTA-LSP for Pb<sup>2+</sup> at 298.15, 308.15, and 318.15 K are 225.88, 212.98, and 204.94 mg g<sup>-1</sup>, respectively. Fig. 6d indicates the excellent adsorption property of EDTA-LSP for MG; the maximum adsorption capacities at 298.15, 308.15, and 318.15 K are 347.87, 318.74, and 310.61 mg g<sup>-1</sup>, respectively. The adsorption capacities of EDTA-LSP toward Pb<sup>2+</sup> and MG decrease with increase of the temperature, which reveals that the adsorptions of both Pb<sup>2+</sup> and MG onto EDTA-LSP are exothermic processes [5]. Furthermore, a comparison of Pb<sup>2+</sup> and/or MG adsorption on EDTA-LSP and many previously reported adsorbents were investigated, and the results are summarized in Table 1. It can be seen that the adsorption capacity of EDTA-LSP for Pb<sup>2+</sup> and MG is higher than those of the mostly listed adsorbents. Moreover, the EDTA-LSP has a distinctive advantage over other adsorbents because it can be used as a dual-use adsorbent for removal of both Pb<sup>2+</sup> and MG.

To depict the processes of Pb<sup>2+</sup> and MG adsorption onto EDTA-LSP, these isothermal adsorption data are fitted by two commonly used theoretical models (i.e., Langmuir and Freundlich models). In general, the Langmuir adsorption model represents adsorbate in solution homogeneously adsorbing onto solid surface by the means of monolayer, whereas the Freundlich adsorption model describes the

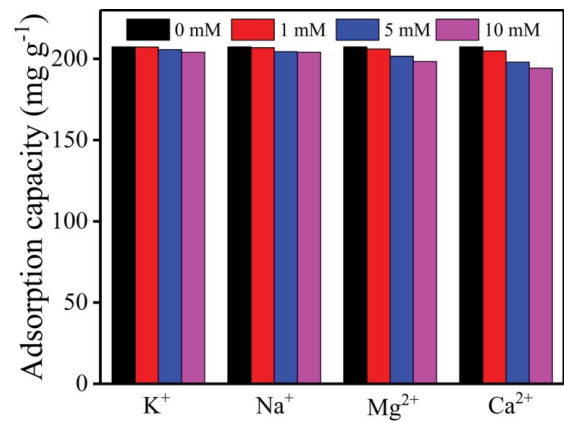


Fig. 5. Effect of common interfering ions on the adsorption capacity of EDTA-LSP for Pb<sup>2+</sup>.

interaction between adsorbate and adsorbent surface in manner of heterogeneous adsorption [8,32]. The linear forms of both theoretical models can be expressed as follows [52]:

$$\frac{1}{q_e} = \frac{1}{q_m} + \frac{1}{K_L q_m C_e} \tag{4}$$

$$\ln q_e = \ln K_F + \frac{1}{n} \ln C_e \tag{5}$$

where C<sub>e</sub> is the equilibrium concentration (mg L<sup>-1</sup>) of Pb<sup>2+</sup> or MG in aqueous solution, respectively; q<sub>e</sub> and q<sub>m</sub> are the equilibrium and maximum adsorption capacities (mg g<sup>-1</sup>) of EDTA-LSP for Pb<sup>2+</sup> or MG, respectively; K<sub>L</sub> is the Langmuir binding constant (L mg<sup>-1</sup>); K<sub>F</sub> (mg<sup>1-1/n</sup> L<sup>1/n</sup> g<sup>-1</sup>) and 1/n are Freundlich constants, respectively.

The linear Langmuir and Freundlich isotherm plots for the adsorption of Pb<sup>2+</sup> and MG onto EDTA-LSP at three temperatures are presented in Fig. 6. Examination of these plots suggests that the linear Langmuir isotherm is a perfect model for the adsorption of Pb<sup>2+</sup> and MG onto EDTA-LSP. Table 2 lists the isotherm parameters (q<sub>m</sub>, K<sub>L</sub>, K<sub>F</sub>, and 1/n) and the coefficients of determinations (R<sup>2</sup>). Comparing these R<sup>2</sup> values, it can be clearly seen that the Langmuir model appears

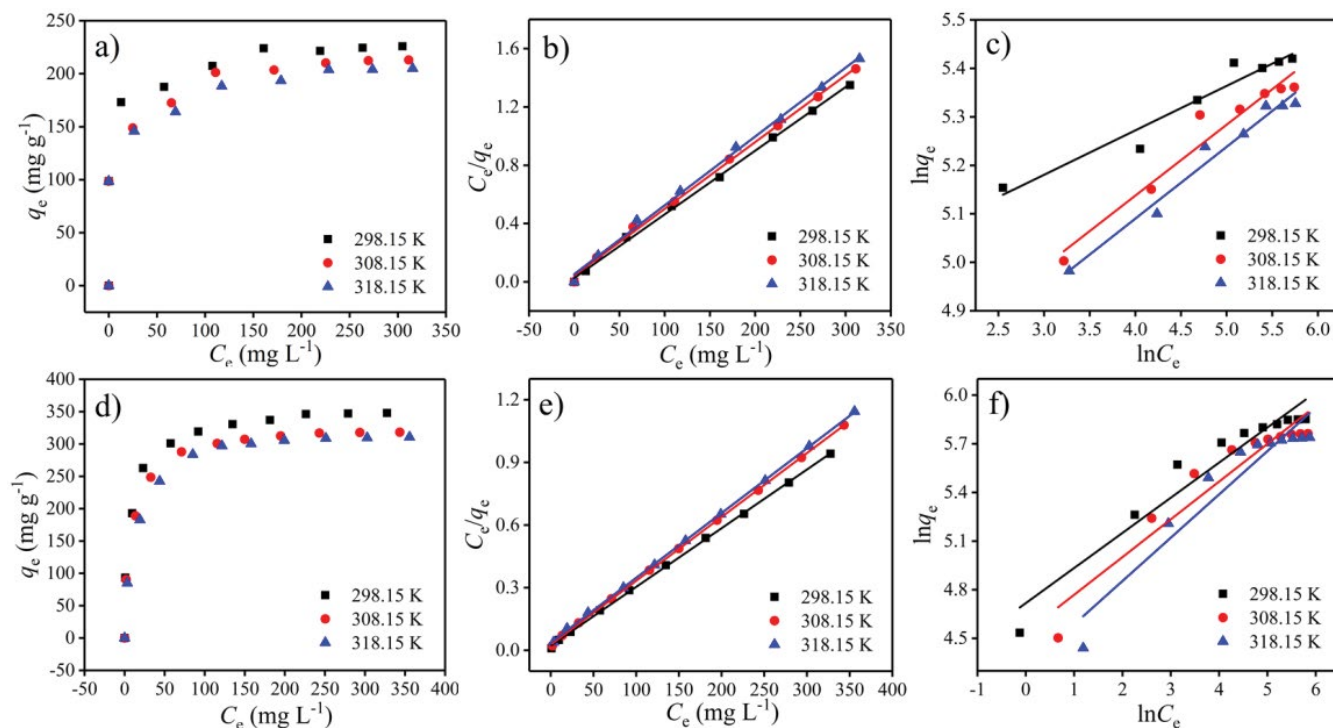


Fig. 6. Effect of temperature on the adsorption capacity of EDTA-LSP toward  $Pb^{2+}$  (a) and MG (d); adsorption isotherm data of  $Pb^{2+}$  and MG onto EDTA-LSP and the fitting plots predicted by Langmuir isotherm (b and e) and Freundlich isotherm (c and f) at three different temperatures.

Table 1  
Comparison on adsorption capacities among various  $Pb^{2+}$  and MG adsorbents

Adsorbents	Modifying agents	$q_{max}$ (mg g <sup>-1</sup> )		pH	References
		$Pb^{2+}$	MG		
<i>Typha angustifolia</i> biomass	EDTA	263.90		5	[42]
Magnetic nanoparticle	EDTA	100.20		7	[25]
Mesoporous silica	EDTA	273.20		5	[43]
Magnetic baker's yeast	EDTA	99.26		5.5	[39]
Chitosan-silica hybrid	EDTA	130.50		3	[44]
$\beta$ -cyclodextrin/chitosan	EDTA	114.80		5	[36]
Cellulose filter paper	EDTA	227.30		7	[32]
Mercedized cellulose	Triethylenetetramine	192.30		6	[27]
Groundnut husk	EDTA		124.80	5	[45]
Ginger waste	H <sub>2</sub> SO <sub>4</sub> and ZnCl <sub>2</sub>		188.60	9	[46]
Rice husk	NaOH		21.32	7	[47]
Magnesium phyllosilicate	Aminopropyl		334.80	9.8	[48]
Fe <sub>3</sub> O <sub>4</sub> -SiO <sub>2</sub> nanorods	Mg(NO <sub>3</sub> ) <sub>2</sub>		125.15	4.8	[49]
Rice straw	Citric acid		256.41	6	[50]
Jute fiber	Phosphoric acid		136.58	8	[51]
Lotus seedpod	EDTA	225.88		5	This work
Lotus seedpod	EDTA		347.87	6	This work

Table 2  
Adsorption isotherm parameters for Pb<sup>2+</sup> and MG adsorption onto EDTA-LSP

Adsorbate	T (K)	$q_{e,exp}$ (mg g <sup>-1</sup> )	Langmuir isotherm model			Freundlich isotherm model		
			$q_m$ (mg g <sup>-1</sup> )	$K_L$ (L mg <sup>-1</sup> )	$R^2$	$K_F$ (mg <sup>1-1/n</sup> L <sup>1/n</sup> g <sup>-1</sup> )	1/n	$R^2$
Pb <sup>2+</sup>	298.15	225.88	228.83	0.1663	0.9985	135.0574	0.0916	0.9316
	308.15	212.98	218.34	0.1067	0.9979	94.8721	0.1463	0.9375
	318.15	204.94	211.86	0.0895	0.9967	89.8085	0.1481	0.9682
MG	298.15	347.87	355.87	0.1257	0.9995	111.8893	0.2167	0.9279
	308.15	318.74	326.80	0.1137	0.9998	93.3429	0.2328	0.9002
	318.15	310.61	322.58	0.0845	0.9998	75.1698	0.2671	0.8940

to produce a more reasonable linear fitting to the experimental data than the Freundlich model. The results manifest that the binding sites (i.e., EDTA) of EDTA-LSP are uniformly distributed on the surface, and the uptakes of Pb<sup>2+</sup> and MG are considered as monolayer adsorptions [53].

### 3.2.5. Adsorption kinetics

Adsorption kinetics can offer important information regarding the adsorption rate and possible pathway of adsorbate uptake on adsorbent, and therefore, in large part determines the potential application of adsorbent. In this study, the relationship between contact time and the adsorption amount of Pb<sup>2+</sup> and MG on EDTA-LSP was studied, and the results are shown in Fig. 7. Obviously, the adsorptions of both Pb<sup>2+</sup> and MG onto EDTA-LSP proceed very fast. For instance, only 30 min is already sufficient for Pb<sup>2+</sup> to reach adsorption equilibrium at all the investigated initial Pb<sup>2+</sup> concentrations (50, 100, and 200 mg L<sup>-1</sup>). Many previous studies showed the equilibrium time for Pb<sup>2+</sup> adsorption on a variety of adsorbents is in the range of 120–300 min, for example, 120 min for rice husk modified by tartaric acid [54], 180 min for peanut husk modified by formalin [55], and 240 min for wood pulp modified by ethylenediamine [56], and 300 min for modified spent coffee grains with citric acid [57]. The required contact time in this study is lower than the bottom value, implying the rapid fast rate of EDTA-LSP. Such rapid binding should be attributed to the highly accessibility of EDTA moieties of EDTA on EDTA-LSP.

Furthermore, pseudo-first-order and pseudo-second-order kinetic models were adopted here in order to understand the kinetic processes in depth [41]. Their linear forms are expressed as follows [52]:

$$\ln(q_e - q_t) = \ln q_e - k_1 t \quad (6)$$

$$\frac{t}{q_t} = \frac{1}{k_2 q_e^2} + \frac{1}{q_e} t \quad (7)$$

where  $q_e$  and  $q_t$  represent the adsorption capacities (mg g<sup>-1</sup>) of EDTA-LSP toward Pb<sup>2+</sup> or MG at equilibrium and at time  $t$  (min), respectively;  $k_1$  (min<sup>-1</sup>) and  $k_2$  (g mg<sup>-1</sup> min<sup>-1</sup>) are the rate constants of pseudo-first-order and pseudo-second-order models, respectively.

Fitting experimental data with above-mentioned kinetic models for initial Pb<sup>2+</sup> concentrations of 50, 100, and 300 mg L<sup>-1</sup> and for initial MG concentrations of 50, 200, and 400 mg L<sup>-1</sup> were performed, and the results are shown in Fig. 7. Intuitively, in all cases, the experimental data are in accordance with the plots predicted by pseudo-second-order model, which implies the applicability of this model for description of these adsorption processes. The kinetic parameters ( $k_1$ ,  $k_2$ ,  $q_{e,calc,1}$ , and  $q_{e,calc,2}$ ) and the corresponding correlation coefficients ( $R^2$ ) were also calculated, and the results are summarized in Table 3. By comparing the  $R^2$  values, it can be found that all these adsorption processes obey pseudo-second-order model rather than pseudo-first-order model. This conclusion is further supported by the fact that the adsorption capacity predicted by pseudo-second-order model ( $q_{e,calc,2}$ ) is very close to the experimentally obtained ( $q_{e,exp}$ ).

### 3.3. Coadsorption behavior and mechanism

Above results indicate the feasibility of EDTA-LSP as an adsorbent for removal of Pb<sup>2+</sup> and MG in single pollutant solutions. In view of the fact that heavy metal ions and organic pollutants commonly coexist in the real wastewaters, it is of significance to further investigate the coadsorption behavior of EDTA-LSP in the coexistence of Pb<sup>2+</sup> and MG. For this purpose, a batch coadsorption experiments were carried out, where removal efficiencies of EDTA-LSP toward Pb<sup>2+</sup> and MG in binary pollutant solutions (pH 5) were determined at a fixed MG concentration (500 mg L<sup>-1</sup>) and varying Pb<sup>2+</sup> concentrations (10–300 mg L<sup>-1</sup>). As shown in Fig. 8, the adsorption capacity of EDTA-LSP toward Pb<sup>2+</sup> was basically unchanged over the entire concentration range of Pb<sup>2+</sup> investigated, despite the presence of highly concentrated MG (500 mg L<sup>-1</sup>) in the solutions. The results indicate that the affinity between EDTA-LSP and Pb<sup>2+</sup> is very strong, which ensures high removal efficiency of EDTA-LSP toward Pb<sup>2+</sup> and can effectively prevent the interference from MG. Interestingly, it is found that the adsorption of EDTA-LSP toward MG is also very effective in binary pollutant systems. When the concentration of Pb<sup>2+</sup> increases from 10 to 300 mg L<sup>-1</sup>, the adsorption capacity of EDTA-LSP toward MG only exhibits a rather limited decrease. This result evidently demonstrates that the EDTA-LSP can serve as a dual-use adsorbent for simultaneous removal of Pb<sup>2+</sup> and MG without significant mutual interference between the two classes of contaminants.

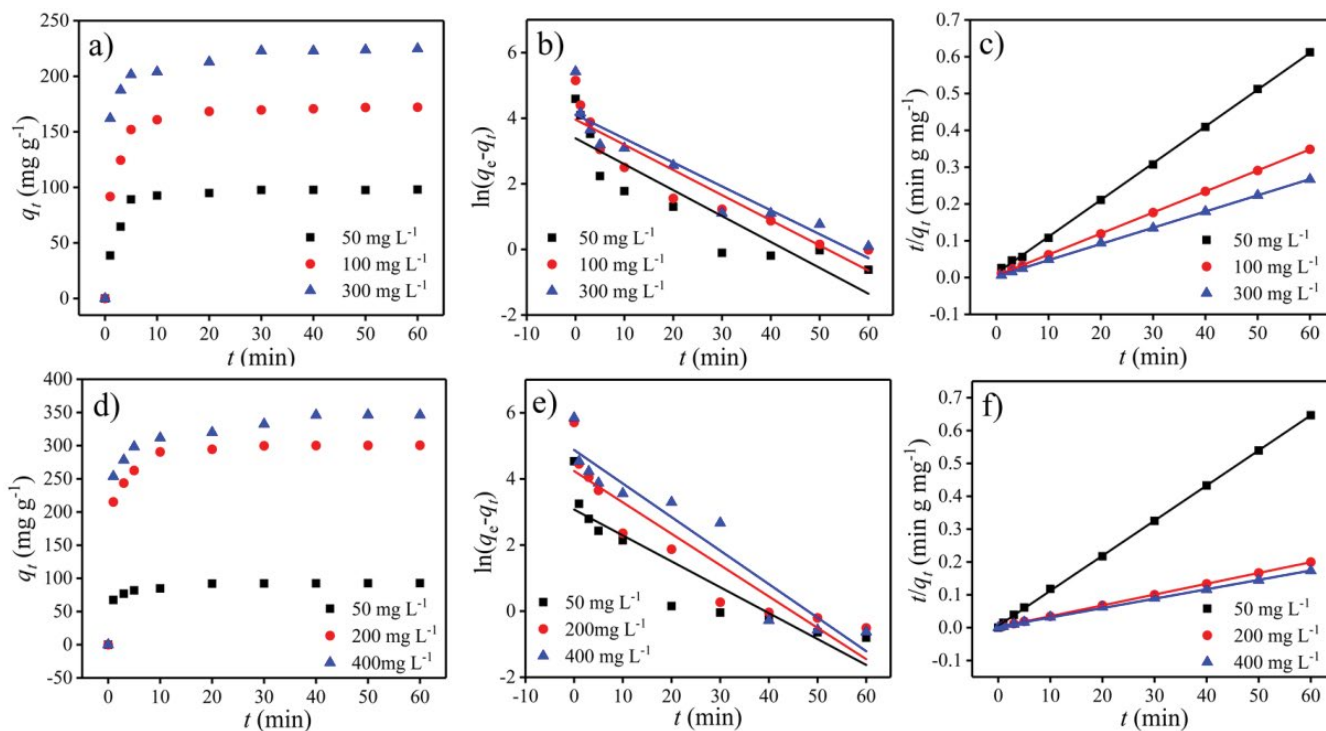


Fig. 7. Effect of contact time on the adsorption capacity of EDTA-LSP toward  $\text{Pb}^{2+}$  (a) and MG (d); adsorption kinetic data of  $\text{Pb}^{2+}$  and MG onto EDTA-LSP and the fitting plots predicted by pseudo-first-order (b and e) and pseudo-second-order (c and f) kinetic models at three different concentrations.

Table 3

Kinetic parameters of pseudo-first-order and pseudo-second-order kinetic models for  $\text{Pb}^{2+}$  and MG adsorption onto EDTA-LSP

Adsorbate	$C_0$ (mg L <sup>-1</sup> )	$q_{e,exp}$ (mg g <sup>-1</sup> )	Pseudo-first-order model			Pseudo-second-order model		
			$k_1$ (min <sup>-1</sup> )	$q_{e,cal,1}$ (mg g <sup>-1</sup> )	$R^2$	$k_2$ (g mg <sup>-1</sup> min <sup>-1</sup> )	$q_{e,cal,2}$ (mg g <sup>-1</sup> )	$R^2$
$\text{Pb}^{2+}$	50	98.56	0.0790	29.60	0.7969	0.0088	100.20	0.9997
	100	173.10	0.0767	52.38	0.8541	0.0062	174.83	0.9999
	300	225.88	0.0729	60.95	0.8675	0.0057	227.27	0.9998
MG	50	92.78	0.0784	21.64	0.8087	0.0212	93.55	0.9998
	200	301.09	0.0949	69.33	0.8536	0.0057	303.95	0.9999
	400	346.26	0.1015	131.04	0.9067	0.0035	349.65	0.9992

In order to understand the coadsorption behavior, a series of characterization analyses were conducted. The XPS analyses were first performed to measure the binding energies of EDTA-LSP and  $\text{Pb}^{2+}$ -adsorbed EDTA-LSP (Fig. 9). As shown in Fig. 9b, the double peaks of Pb 4f orbital at 138.78 and 143.48 eV appear in  $\text{Pb}^{2+}$ -adsorbed EDTA-LSP, which confirms the successful adsorption of  $\text{Pb}^{2+}$  ions by EDTA-LSP adsorbent. Fig. 9c shows the O 1s spectra of EDTA-LSP and  $\text{Pb}^{2+}$ -adsorbed EDTA-LSP. The binding energy of O 1s for the EDTA-LSP is 532.38 eV, which shifts to 532.88 eV after the  $\text{Pb}^{2+}$  adsorption. This change signifies the contribution of carboxyl groups to  $\text{Pb}^{2+}$  adsorption [39]. The same tendency is also found in the N 1s spectra of EDTA-LSP and  $\text{Pb}^{2+}$ -adsorbed EDTA-LSP (Fig. 9d), indicating that the nitrogen atoms could share electrons with  $\text{Pb}^{2+}$ . Furthermore, the C 1s XPS spectra of EDTA-LSP

and  $\text{Pb}^{2+}$ -adsorbed EDTA-LSP are compared. As shown in Fig. 9e, the C 1s spectrum of EDTA-LSP can be deconvoluted into four peaks with differentiated binding energy values, which can be attributed to the carbon atoms in the forms of C–C (284.33 eV), C–N (285.73 eV), C=O (286.55 eV), and O=C–O (288.19 eV), respectively [58]. After  $\text{Pb}^{2+}$  uptake, the peaks of C–C (284.79 eV) and C=O (286.44 eV) remain almost unchanged, while the peaks of C–N (285.62 eV) disappears and the binding energy of O=C–O (288.61 eV) changes (Fig. 9f), which is on behalf of the contributions of C–N and O=C–O to the formation of Pb complexation. Based on these XPS survey results, it can be inferred that the adsorption of  $\text{Pb}^{2+}$  onto EDTA-LSP is driven by the surface complexation between EDTA and  $\text{Pb}^{2+}$ , where the O and N of EDTA act as coordination atoms responsible for the binding of  $\text{Pb}^{2+}$ .

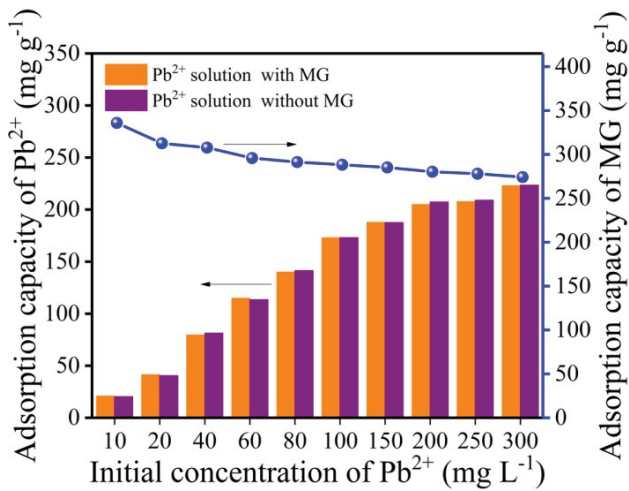


Fig. 8. Coadsorption behaviors of  $Pb^{2+}$  and MG onto EDTA-LSP at pH 5.

Fig. S1 shows FT-IR spectra of MG, EDTA-LSP,  $Pb^{2+}$ -adsorbed EDTA-LSP, and MG-adsorbed EDTA-LSP. It is observed that the characteristic peak of carboxyl groups shifts obviously from 1,644.9 to 1,583.8  $cm^{-1}$  after  $Pb^{2+}$  adsorption, which further confirms the formation of coordination interaction between the carboxyl groups and  $Pb^{2+}$  ions. Meanwhile, a new peak at 1,170.3  $cm^{-1}$  appears after

MG adsorption, indicating that MG can be also effectively adsorbed onto the EDTA-LSP. Moreover, by carefully comparing the FT-IR spectra of EDTA-LSP and MG-adsorbed EDTA-LSP (Fig. S1), it can be seen that the characteristic peak of MG does not exhibit any shift in wavenumber, implying that the MG adsorption onto EDTA-LSP is driven by electrostatic interaction instead of chemical binding.

Fig. S2 gives the zeta potential values of EDTA-LSP,  $Pb^{2+}$ -adsorbed EDTA-LSP, and  $Pb^{2+}$ -MG-coadsorbed EDTA-LSP at pH 5. Clearly, the zeta potential of EDTA-LSP is significantly negative, which should be attributed to easy deprotonation of the carboxyl groups of EDTA-LSP under such conditions. After  $Pb^{2+}$  uptake, the obtained  $Pb^{2+}$ -adsorbed EDTA-LSP is still negatively charged, and the magnitude of its zeta potential is close to that of EDTA-LSP (Fig. S2). This result implies that when  $Pb^{2+}$  ions bind to the EDTA moieties on EDTA-LSP, the resulting EDTA- $Pb^{2+}$  complexes exist in the anionic form. After further adsorption of MG onto the  $Pb^{2+}$ -adsorbed EDTA-LSP, the  $Pb^{2+}$ -MG-coadsorbed EDTA-LSP has a nearly neutral zeta potential (Fig. S2). This should be due to the shielding effect of cationic MG on the negatively charged  $Pb^{2+}$ -adsorbed EDTA-LSP.

Based on above-mentioned characterization results, a possible coadsorption mechanism is proposed (Scheme 2). When  $Pb^{2+}$  and MG coexist in an aqueous solution, the  $Pb^{2+}$  can be preferentially adsorbed onto EDTA-LSP via a strong surface complexation process. Notably, the formed EDTA- $Pb^{2+}$  complexes on the EDTA-LSP surface are negatively charged,

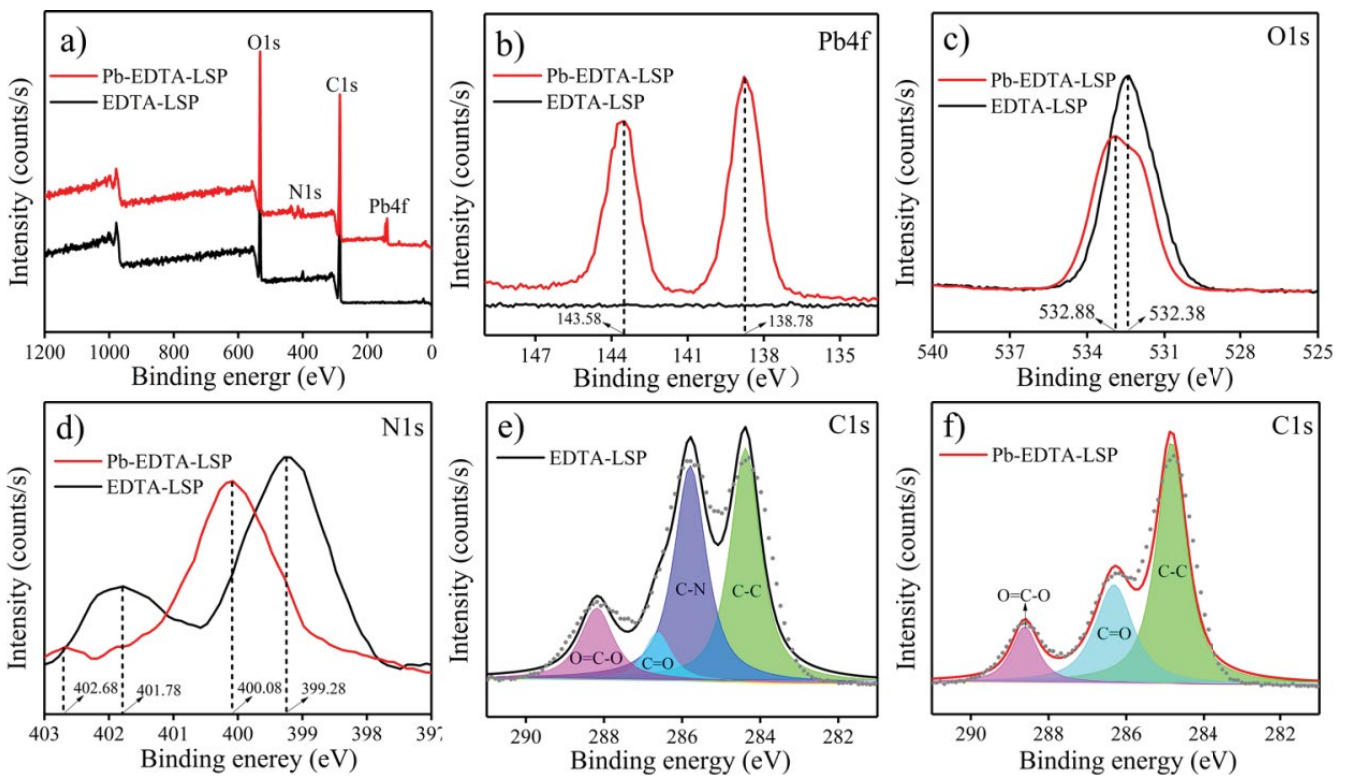
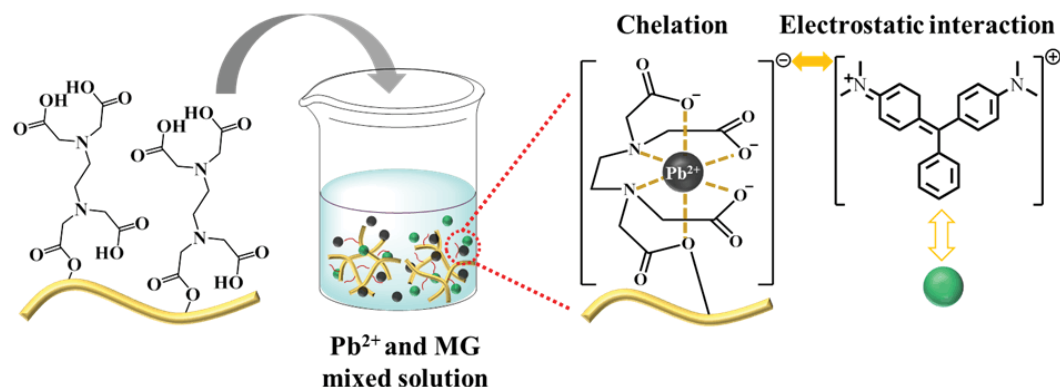


Fig. 9. XPS spectra of EDTA-LSP and  $Pb^{2+}$ -adsorbed EDTA-LSP: (a) wide scanning spectra of EDTA-LSP and  $Pb^{2+}$ -adsorbed EDTA-LSP; (b) Pb 4f spectra of EDTA-LSP and  $Pb^{2+}$ -adsorbed EDTA-LSP; (c) O 1s spectra of EDTA-LSP and  $Pb^{2+}$ -adsorbed EDTA-LSP; (d) N 1s spectra of EDTA-LSP and  $Pb^{2+}$ -adsorbed EDTA-LSP; (e) C 1s spectra of EDTA-LSP; (f) C 1s spectra of  $Pb^{2+}$ -adsorbed EDTA-LSP.



Scheme 2. Coadsorption mechanism of Pb<sup>2+</sup> and MG onto EDTA-LSP.

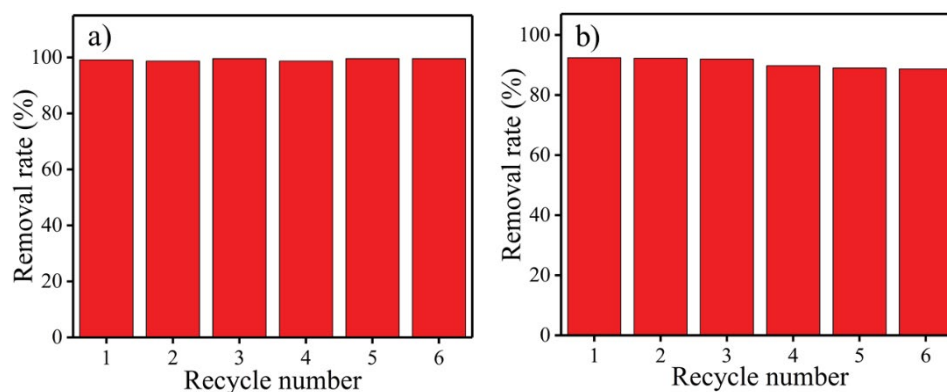


Fig. 10. Reusability of EDTA-LSP for Pb<sup>2+</sup> (a) and MG (b) removal.

which can subsequently act as effective adsorption sites for capturing cationic MG from aqueous solution via electrostatic interaction. Benefitting from the differential binding behaviors, the competition between Pb<sup>2+</sup> and MG can be largely reduced and a satisfying coadsorption is therefore achieved.

### 3.4. Reusability of EDTA-LSP

Reusability of solid adsorbent is well-known to be an imperative factor for evaluating its potential practical application. Thus, further attempt was made by us to reuse the exhausted EDTA-LSP after regeneration by elution, where EDTA aqueous solution (0.1 mol L<sup>-1</sup>; pH 4.5) and CH<sub>2</sub>CH<sub>3</sub>OH–H<sub>2</sub>O mixture (v/v = 1:1; pH 2) were used as eluents for desorption of the adsorbed Pb<sup>2+</sup> and MG, respectively. The removal efficiencies of EDTA-LSP for Pb<sup>2+</sup> and MG under different reuse cycles are shown in Fig. 10. It can be seen that the removal rate for Pb<sup>2+</sup> is nearly 100% in the first cycle and still reaches 98.7% after six cycles (Fig. 10a). The effectiveness of EDTA aqueous solution for Pb<sup>2+</sup> desorption should be ascribed to the strong chelating interaction between EDTA and Pb<sup>2+</sup>, which contributes to a facile release of Pb<sup>2+</sup> ions from the EDTA-LSP surface to bulk solution. Fig. 10b presents the cycle-dependent removal efficiency of EDTA-LSP for MG. It is clearly observed that the

EDTA-LSP retains 96% of its initial removal rate after six cycles, indicating that the employed acidic ethanol solution is sufficiently effective for MG desorption. This should be in large part due to the principle of compatibility between similar species. Moreover, use of acidic solution to regenerate carboxyl groups on adsorbent surface is also in favor of weakening electrostatic interaction and facilitating the elution of MG from adsorption sites [59–61]. The satisfactory recycling performance of EDTA-LSP reflects that the covalent grafting of EDTA moieties onto LSP is stable enough to avoid the leaching of active sites during reuse. All these investigations indicate that the EDTA-LSP should be sustainably used for the adsorptive removal of heavy metal ions and organic pollutants from wastewaters.

## 4. Conclusions

In summary, a novel EDTA-modified agricultural by-product (EDTA-LSP) was facilely fabricated based on the covalent grafting of abundant EDTA moieties onto the LSP, and its intrinsic adsorption and coadsorption properties in the removal of Pb<sup>2+</sup> and MG were elucidated. Batch adsorption investigations indicated that the EDTA-LSP was highly efficient for adsorptive removal of Pb<sup>2+</sup> and MG from single pollutant systems, exhibiting considerably high adsorption capacities (Pb<sup>2+</sup>: 225.88 mg g<sup>-1</sup>; MG: 347.87 mg g<sup>-1</sup>) and

rapid kinetics. More importantly, when used in Pb<sup>2+</sup>–MG binary systems, the EDTA-LSP exhibited unique differential binding behaviors. The surface EDTA moieties preferentially bound with Pb<sup>2+</sup>, and then the formed EDTA–Pb<sup>2+</sup> complexes carrying negative charge could effectively adsorb cationic MG, which led to a less competitive and quite satisfying coadsorption. Moreover, this adsorbent could remain high and stable removal efficiencies for Pb<sup>2+</sup> and MG during reuse. Findings from this study may help the development of inexpensive but efficient methods that can be applicable to complex wastewater treatment. Moreover, the gained insight into the unique coadsorption properties of EDTA-LSP should have implications for understanding the binding process that occurred between a mono-site host material and multiple guest species.

### Acknowledgments

The authors acknowledge the research grant provided by National Key R&D Program of China (No. 2018YFF0215404 and 2018YFF0215402), National Natural Science Foundation of China (No. 41690131), Fundamental Research Funds for the Central Universities, China University of Geosciences (Wuhan) (No. CUG170101), and General Administration of Quality Supervision, Inspection, and Quarantine of China (No. 2015IK217).

### References

- [1] E.I. Unuabonah, C. Günter, J. Weber, S. Lubahn, A. Taubert, Hybrid clay: a new highly efficient adsorbent for water treatment, *ACS Sustainable Chem. Eng.*, 1 (2013) 966–973.
- [2] J.Y. Lim, N.M. Mubarak, E.C. Abdullah, S. Nizamuddin, M. Khalid, Recent trends in the synthesis of graphene and graphene oxide based nanomaterials for removal of heavy metals—a review, *J. Ind. Eng. Chem.*, 66 (2018) 29–44.
- [3] G.S. Ibrahim, A.M. Isloor, A.M. Asiri, A.F. Ismail, R. Kumar, M.I. Ahamed, Performance intensification of the polysulfone ultrafiltration membrane by blending with copolymer encompassing novel derivative of poly (styrene-co-maleic anhydride) for heavy metal removal from wastewater, *Chem. Eng. J.*, 353 (2018) 425–435.
- [4] V.K. Gupta, A. Nayak, S. Agarwal, Bioadsorbents for remediation of heavy metals: current status and their future prospects, *Environ. Eng. Res.*, 20 (2015) 1–18.
- [5] Z.A. Al-Othman, R. Ali, M. Naushad, Hexavalent chromium removal from aqueous medium by activated carbon prepared from peanut shell: adsorption kinetics, equilibrium and thermodynamic studies, *Chem. Eng. J.*, 184 (2012) 238–247.
- [6] M. Naushad, S. Vasudevan, G. Sharma, A. Kumar, Z.A. Al-Othman, Adsorption kinetics, isotherms, and thermodynamic studies for Hg<sup>2+</sup> adsorption from aqueous medium using alizarin red-S-loaded amberlite IRA-400 resin, *Desal. Water Treat.*, 57 (2016) 18551–18559.
- [7] F. Zhao, E. Repo, D. Yin, Y. Meng, S. Jafari, M. Sillanpää, EDTA-cross-linked  $\beta$ -cyclodextrin: an environmentally friendly bifunctional adsorbent for simultaneous adsorption of metals and cationic dyes, *Environ. Sci. Technol.*, 49 (2015) 10570–10580.
- [8] J. Wu, J. Zhou, S. Zhang, A. Alsaedi, T. Hayat, J. Li, Y. Song, Efficient removal of metal contaminants by EDTA modified MOF from aqueous solutions, *J. Colloid Interface Sci.*, 555 (2019) 403–412.
- [9] C. Zhou, Q. Wu, T. Lei, I.I. Negulescu, Adsorption kinetic and equilibrium studies for methylene blue dye by partially hydrolyzed polyacrylamide/cellulose nanocrystal nanocomposite hydrogels, *Chem. Eng. J.*, 251 (2014) 17–24.
- [10] B.H. Hameed, A.M. Din, A.L. Ahmad, Adsorption of methylene blue onto bamboo-based activated carbon: kinetics and equilibrium studies, *J. Hazard. Mater.*, 141 (2017) 819–825.
- [11] Ö. Etcı, N. Bektaş, M.S. Öncel, Single and binary adsorption of lead and cadmium ions from aqueous solution using the clay mineral beidellite, *Environ. Earth Sci.*, 61 (2010) 231–240.
- [12] M. Monier, D.M. Ayad, Y. Wei, A.A. Sarhan, Adsorption of Cu(II), Co(II), and Ni(II) ions by modified magnetic chitosan chelating resin, *J. Hazard. Mater.*, 177 (2010) 962–970.
- [13] W. Yang, P. Ding, L. Zhou, J. Yu, X. Chen, F. Jiao, Preparation of diamine modified mesoporous silica on multi-walled carbon nanotubes for the adsorption of heavy metals in aqueous solution, *Appl. Surf. Sci.*, 282 (2013) 38–45.
- [14] M. Ahmaruzzaman, Industrial wastes as low-cost potential adsorbents for the treatment of wastewater laden with heavy metals, *Adv. Colloid Interface Sci.*, 166 (2011) 36–59.
- [15] F.M. Pelleria, A. Giannis, D. Kalderis, K. Anastasiadou, R. Stegmann, J.Y. Wang, E. Gidarakos, Adsorption of Cu(II) ions from aqueous solutions on biochars prepared from agricultural by-products, *J. Environ. Manage.*, 96 (2012) 35–42.
- [16] H.R. Mahmoud, S.M. Ibrahim, S.A. El-Molla, Textile dye removal from aqueous solutions using cheap MgO nanomaterials: adsorption kinetics, isotherm studies and thermodynamics, *Adv. Powder Technol.*, 27 (2016) 223–231.
- [17] T.A.H. Nguyen, H.H. Ngo, W.S. Guo, J. Zhang, S. Liang, Q.Y. Yue, T.V. Nguyen, Applicability of agricultural waste and by-products for adsorptive removal of heavy metals from wastewater, *Bioresour. Technol.*, 148 (2013) 574–585.
- [18] M.A.M. Salleh, D.K. Mahmoud, W.A. Karim, A. Idris, Cationic and anionic dye adsorption by agricultural solid wastes: a comprehensive review, *Desalination*, 280 (2011) 1–13.
- [19] R. Han, L. Zhang, C. Song, M. Zhang, H. Zhu, L. Zhang, Characterization of modified wheat straw, kinetic and equilibrium study about copper ion and methylene blue adsorption in batch mode, *Carbohydr. Polym.*, 79 (2010) 1140–1149.
- [20] A.A. El-Bindary, A.Z. El-Sonbati, A.A. Al-Sarawy, K.S. Mohamed, M.A. Farid, Adsorption and thermodynamic studies of hazardous azocoumarin dye from an aqueous solution onto low cost rice straw based carbons, *J. Mol. Liq.*, 199 (2014) 71–78.
- [21] S. Vafakhah, M.E. Bahrololoom, R. Bazarganlari, M. Saeedikhani, Removal of copper ions from electroplating effluent solutions with native corn cob and corn stalk and chemically modified corn stalk, *J. Environ. Chem. Eng.*, 2 (2014) 356–361.
- [22] M.R. Lasheen, N.S. Ammar, S.H. Ibrahim, Adsorption/desorption of Cd(II), Cu(II) and Pb(II) using chemically modified orange peel: equilibrium and kinetic studies, *Solid State Sci.*, 14 (2012) 202–210.
- [23] J. Anwar, U. Shafique, M. Salman, A. Dar, S. Anwar, Removal of Pb(II) and Cd(II) from water by adsorption on peels of banana, *Bioresour. Technol.*, 101 (2010) 1752–1755.
- [24] A. Witek-Krowiak, R.G. Szafran, S. Modelski, Biosorption of heavy metals from aqueous solutions onto peanut shell as a low-cost biosorbent, *Desalination*, 265 (2011) 126–134.
- [25] Y. Huang, A.A. Keller, EDTA functionalized magnetic nanoparticle sorbents for cadmium and lead contaminated water treatment, *Water Res.*, 80 (2015) 159–168.
- [26] M. Najafi, Y. Yousefi, A.A. Rafati, Synthesis, characterization and adsorption studies of several heavy metal ions on amino-functionalized silica nano hollow sphere and silica gel, *Sep. Purif. Technol.*, 85 (2012) 193–205.
- [27] L.V.A. Gurgel, L.F. Gil, Adsorption of Cu(II), Cd(II), and Pb(II) from aqueous single metal solutions by succinylated mercerized cellulose modified with triethylenetetramine, *Carbohydr. Polym.*, 77 (2009) 142–149.
- [28] Y. Zhang, Y. Li, L.Q. Yang, X.J. Ma, L.Y. Wang, Z.F. Ye, Characterization and adsorption mechanism of Zn<sup>2+</sup> removal by PVA/EDTA resin in polluted water, *J. Hazard. Mater.*, 178 (2010) 1046–1054.
- [29] O.K. Júnior, L.V.A. Gurgel, R.P. de Freitas, L.F. Gil, Adsorption of Cu(II), Cd(II), and Pb(II) from aqueous single metal solutions by mercerized cellulose and mercerized sugarcane bagasse

- chemically modified with EDTA dianhydride (EDTAD), Carbohydr. Polym., 77 (2009) 643–650.
- [30] Q. He, H. Wang, J. Zhang, Z. Zou, J. Zhou, K. Yang, L. Zheng, Lotus seedpod as a low-cost biomass for potential methylene blue adsorption, Water Sci. Technol., 74 (2016) 2560–2568.
- [31] Y. Li, L. Hu, B. Shen, C. Dai, Q. Xu, D. Liu, M. Xu, Rib-like hierarchical porous carbon as reservoir for long-life and high-rate Li-Te batteries, Electrochim. Acta, 250 (2017) 10–15.
- [32] M. d'Halluin, J. Rull-Barrull, G. Bretel, C. Labrugère, E. Le Grogneq, F.X. Felpin, Chemically modified cellulose filter paper for heavy metal remediation in water, ACS Sustainable Chem. Eng., 5 (2017) 1965–1973.
- [33] L. Cui, Y. Wang, L. Gao, L. Hu, L. Yan, Q. Wei, B. Du, EDTA functionalized magnetic graphene oxide for removal of Pb(II), Hg(II) and Cu(II) in water treatment: adsorption mechanism and separation property, Chem. Eng. J., 281 (2015) 1–10.
- [34] A.C. Leon, Q. Chen, N.B. Palaganas, J.O. Palaganas, J. Manapat, R.C. Advincula, High performance polymer nanocomposites for additive manufacturing applications, React. Funct. Polym., 103 (2016) 141–155.
- [35] W. Zhang, H. Li, X. Kan, L. Dong, H. Yan, Z. Jiang, R. Cheng, Adsorption of anionic dyes from aqueous solutions using chemically modified straw, Bioresour. Technol., 117 (2012) 40–47.
- [36] D. Wu, L. Hu, Y. Wang, Q. Wei, L. Yan, T. Yan, B. Du, EDTA modified  $\beta$ -cyclodextrin/chitosan for rapid removal of Pb(II) and acid red from aqueous solution, J. Colloid Interface Sci., 523 (2018) 56–64.
- [37] Y. Zhou, M. Zhang, X. Hu, X. Wang, J. Niu, T. Ma, Adsorption of cationic dyes on a cellulose-based multicarboxyl adsorbent, J. Chem. Eng. Data, 58 (2013) 413–421.
- [38] N. Tewari, P. Vasudevan, B.K. Guha, Study on biosorption of Cr(VI) by *Mucor hiemalis*, Biochem. Eng. J., 23 (2005) 185–192.
- [39] Y. Zhang, J. Zhu, L. Zhang, Z. Zhang, M. Xu, M. Zhao, Synthesis of EDTAD-modified magnetic baker's yeast biomass for Pb<sup>2+</sup> and Cd<sup>2+</sup> adsorption, Desalination, 278 (2011) 42–49.
- [40] X.J. Li, C.J. Yan, W.J. Luo, Q. Gao, Q. Zhou, C. Liu, S. Zhou, Exceptional cerium(III) adsorption performance of poly (acrylic acid) brushes-decorated attapulgite with abundant and highly accessible binding sites, Chem. Eng. J., 284 (2016) 333–342.
- [41] S. Chakraborty, S. Chowdhury, P.D. Saha, Adsorption of crystal violet from aqueous solution onto NaOH-modified rice husk, Carbohydr. Polym., 86 (2011) 1533–1541.
- [42] W.J. Liu, F.X. Zeng, H. Jiang, X.S. Zhang, Adsorption of lead (Pb) from aqueous solution with Typha angustifolia biomass modified by SOCl<sub>2</sub> activated EDTA, Chem. Eng. J., 170 (2011) 21–28.
- [43] J. Huang, M. Ye, Y. Qu, L. Chu, R. Chen, Q. He, D. Xu, Pb(II) removal from aqueous media by EDTA-modified mesoporous silica SBA-15, J. Colloid Interface Sci., 385 (2012) 137–146.
- [44] E. Repo, J.K. Warchol, A. Bhatnagar, M. Sillanpää, Heavy metals adsorption by novel EDTA-modified chitosan–silica hybrid materials, J. Colloid Interface Sci., 358 (2011) 261–267.
- [45] B.J. Titilayo, B.A. Adesina, N.M. Olubunmi, A.S. Akinyeye, I.A. Ayodeji, Kinetics and thermodynamic studies of adsorption of malachite green onto unmodified and EDTA-modified groundnut husk, Afr. J. Pure Appl. Chem., 6 (2012) 141–152.
- [46] R. Ahmad, R. Kumar, Adsorption studies of hazardous malachite green onto treated ginger waste, J. Environ. Manage., 91 (2010) 1032–1038.
- [47] S. Chowdhury, R. Mishra, P. Saha, P. Kushwaha, Adsorption thermodynamics, kinetics and isosteric heat of adsorption of malachite green onto chemically modified rice husk, Desalination, 265 (2011) 159–168.
- [48] Y.C. Lee, E.J. Kim, J.W. Yang, H.J. Shin, Removal of malachite green by adsorption and precipitation using aminopropyl functionalized magnesium phyllosilicate, J. Hazard. Mater., 192 (2011) 62–70.
- [49] H. Liu, Z. Mo, L. Li, F. Chen, Q. Wu, L. Qi, Efficient removal of copper(II) and malachite green from aqueous solution by magnetic magnesium silicate composite, J. Chem. Eng. Data, 62 (2017) 3036–3042.
- [50] R. Gong, Y. Jin, F. Chen, J. Chen, Z. Liu, Enhanced malachite green removal from aqueous solution by citric acid modified rice straw, J. Hazard. Mater., 137 (2016) 865–870.
- [51] K. Porkodi, K.V. Kumar, Equilibrium, kinetics and mechanism modeling and simulation of basic and acid dyes sorption onto jute fiber carbon: eosin yellow, malachite green and crystal violet single component systems, J. Hazard. Mater., 143 (2007) 311–327.
- [52] Q. Gao, H. Zhu, W.J. Luo, S. Wang, C.G. Zhou, Preparation, characterization, and adsorption evaluation of chitosan-functionalized mesoporous composites, Microporous Mesoporous Mater., 193 (2014) 15–26.
- [53] Q. Gao, J.F. Xie, Y.T. Shao, C. Chen, B. Han, K.S. Xia, C.G. Zhou, Ultrafast and high-capacity adsorption of Gd(III) onto inorganic phosphorous acid modified mesoporous SBA-15, Chem. Eng. J., 313 (2017) 197–206.
- [54] K. Wong, C. Lee, K. Low, M. Haron, Removal of Cu and Pb by tartaric acid modified rice husk from aqueous solutions, Chemosphere, 50 (2003) 23–28.
- [55] Q. Li, J. Zhai, W. Zhang, M. Wang, J. Zhou, Kinetic studies of adsorption of Pb(II), Cr(III) and Cu(II) from aqueous solution by sawdust and modified peanut husk, J. Hazard. Mater., 141 (2007) 163–167.
- [56] S.M. Musyoka, J.C. Ngila, B. Moodley, L. Petrik, A. Kindness, Synthesis, characterization, and adsorption kinetic studies of ethylenediamine modified cellulose for removal of Cd and Pb, Anal. Lett., 44 (2011) 1925–1936.
- [57] F.J. Cerino-Córdova, P.E. Díaz-Flores, R.B. García-Reyes, E. Soto-Regalado, R. Gómez-González, M.T. Garza-González, E. Bustamante-Alcántara, Biosorption of Cu(II) and Pb(II) from aqueous solutions by chemically modified spent coffee grains, Int. J. Environ. Sci. Technol., 10 (2013) 611–622.
- [58] S.F. Lim, Y.M. Zheng, S.W. Zou, J.P. Chen, Characterization of copper adsorption onto an alginate encapsulated magnetic sorbent by a combined FT-IR, XPS, and mathematical modeling study, Environ. Sci. Technol., 42 (2008) 2551–2556.
- [59] Y. Zhou, M. Zhang, X. Wang, Q. Huang, Y. Min, T. Ma, J. Niu, Removal of crystal violet by a novel cellulose-based adsorbent: comparison with native cellulose, Ind. Eng. Chem. Res., 53 (2014) 5498–5506.
- [60] W.W. Ngah, L.C. Teong, M.A.K.M. Hanafiah, Adsorption of dyes and heavy metal ions by chitosan composites: a review, Carbohydr. Polym., 83 (2011) 1446–1456.
- [61] C. Shen, Y. Shen, Y. Wen, H. Wang, W. Liu, Fast and highly efficient removal of dyes under alkaline conditions using magnetic chitosan-Fe(III) hydrogel, Water. Res., 45 (2011) 5200–5210.

Supplementary information

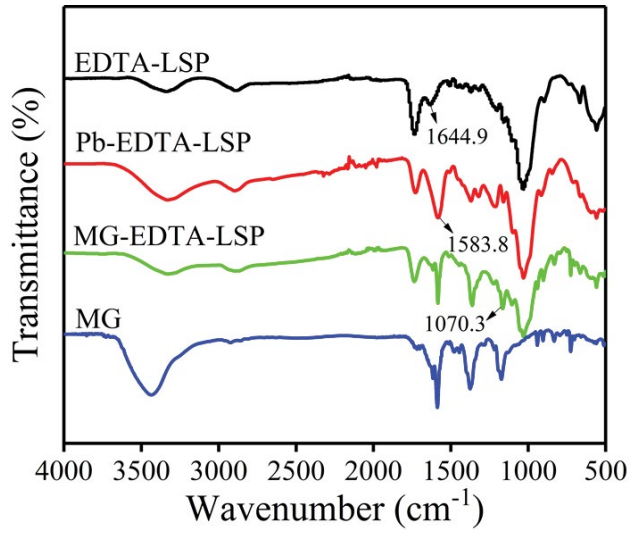


Fig. S1. FT-IR spectra of MG, EDTA-LSP, Pb<sup>2+</sup>-adsorbed EDTA-LSP, and MG-adsorbed EDTA-LSP.

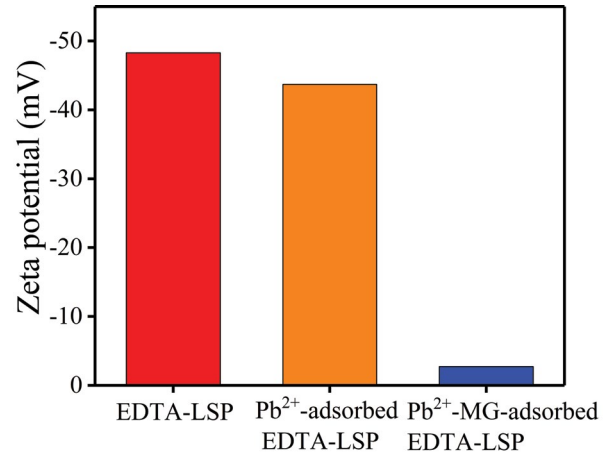


Fig. S2. Comparison of zeta potential values of EDTA-LSP (red bar), Pb<sup>2+</sup>-adsorbed EDTA-LSP (orange bar), and Pb<sup>2+</sup>-MG-adsorbed EDTA-LSP (blue bar) at pH 5.